Research on Engineering Structures & Materials
www.jresm.org
MIM Research Group

Research Article

Enhancing the Goldberg–Richard model with a calibrated influence factor for superior moment–curvature prediction in RC beams

Safaa I. Ali [*,1,a], Omar T. N. Al-Tikrity [2,b], Fatimah A. K. Khattab [2,c], Samah Ahmed Hardan [2,d]

[1]*Dept. of Civil Eng., College of Engineering, University of Samarra, Samarra, Salah Al Deen, Iraq*
[2]*Dept. of Civil Eng., College of Engineering, Tikrit University, Tikrit, Salah Al Deen, Iraq*

Article Info

Article History:

Received 18 Apr 2026

Accepted 04 June 2026

Keywords:

Moment–curvature relationship;
Reinforced concrete beams;
Goldberg–Richard model;
Nonlinear analysis;
Dimensional analysis;
Calibration;
Material interaction

Abstract

The relationship between moment (M) and curvature (κ) is key to characterising nonlinear flexural behaviour of concrete members. This research develops a new method for enhancing predictive accuracy of the Goldberg and Richard (G-R) Power Law model for predicting the behaviour of concrete under compression using a newly developed calibrated influence factor (CIF). Although the G-R model can provide continuous representations of the nonlinearity of the material, predictive accuracy is limited by the complex nature of design variables for composite members. In order to improve predictive accuracy, dimensional analysis and multivariate nonlinear regression analyses were conducted available experimental database to create a dimension-less CIF based on the Material Interaction Index (MII), which represents the mechanical interaction between steel reinforcement and concrete. Use of the CIF in a closed-form sectional analysis provided a means to enhance the prediction of moment response at ultimate strength. Validation of the CIF was performed against two independent programs and beam test results; results showed the CIF provided significant reductions in mean absolute error (MAE), improvements in root mean square error (RMSE), and R^2 values greater than 0.99, while maintaining analytical efficiency for performance based design applications.

1. Introduction

The relationship between moment and curvature (moment-curvature) is necessary for understanding how a reinforced concrete beam will respond when being bent (flexing) or twisted (bending) under load. For example; how much the beam will deflect; how many cracks it will develop; and how much rotational ductility it will exhibit when it reaches its ultimate capacity [1-3]. The accurate prediction of the moment-curvature relationship is critical to the design of structures to meet performance-based criteria, evaluation of serviceability, and determination of the residual capacity of existing structures [4]. Due to the non-linear, inelastic, and path dependent behaviour of the materials (concrete in compression and steel reinforcement in tension), predicting the moment-curvature relationship can be difficult to achieve.

To make calculations easier, some of today's design codes, including IS 456:2000 [5] and Eurocode 2 [6], have simplified the models used to describe the behaviour of concrete and steel. Most of these models describe the stress-strain behaviour of steel using an elastic-perfectly plastic model and the stress-strain behaviour of concrete using a simple stress block (for example, parabolic-rectangle or equivalent rectangular stress block). These simplifications make it easier to perform calculations,

*Corresponding author: safaa.ib.ali@uosamarra.edu.iq
[a]orcid.org/0009-0008-6675-5525; [b]orcid.org/0000-0001-9407-4841; [c]orcid.org/ 0000-0003-4787-0567;
[d]orcid.org/0009-0001-7377-0407
DOI: http://dx.doi.org/10.17515/resm2026-1620st0418rs

and they may provide reasonably accurate estimates of the strength of concrete and steel under load. However, they can also fail to account for the deterioration in stiffness that occurs after cracking, the gradual transition from linear to nonlinear behaviour of concrete as it approaches its peak strength, and the postyield behaviour of steel [7]. While predictions about serviceability limits, deformation capacity, and the ability to absorb energy may be significantly different from what they should be based on actual behaviour.

Advanced numerical methodologies, such as fibre-section analysis and non-linear FEM utilize complex constitutive (uniaxial) relationships in order to produce accurate solutions [8]. The G-R Power Law model [9], which represents the full compressive response of concrete, represents a simple and smooth analytical expression of the stress-strain relationship. As one of the foundations for nonlinear concrete modelling, the G-R model first introduced by Goldberg and Richard in 1963 has undergone significant development by later researchers through new techniques and enhancements to moment–curvature analysis based on fibre-section methods, advancements in constitutive assumptions, and improved analytical methods to enhance the prediction of reinforced concrete (RC) beam behaviour [16,17]. As the compressive response of concrete does not exhibit an explicit peak, and this distributed nature of damage can be captured by the G-R Power Law model. The migration from the research and analytical world into practical design applications of these models has been hampered by the lack of detail surrounding the limitations and inaccuracy associated with the predictive capabilities of models like G-R in terms of material and geometric parameters of RC cross sections. The primary parameters affecting the predictive accuracy of G-R are concrete compressive strength (f^' c), steel yield strength (fy) and tensile reinforcement ratio (ρ). The interaction between these parameters is often neglected or poorly understood, leading to a misconception that the constitutive model behaves as a “blackbox” [10-12].

The study suggests that the interaction between tensile force capacity of reinforcement (ρfy) and compressive strength of concrete (f'c), is the main governing factor of the resultant shaping of the enhanced moment–curvature (M–κ) response. This interaction, therefore, defines the neutral axis depth of a beam as well as the amount of nonlinearity within that concrete element, as well as the point of yielding of the reinforcement and crushing of the concrete. To bridge the newly identified gap, an approach to correcting for the interaction of the two materials was developed through the introduction of a dimensionless Calibrated Influence Factor (CIF), created using dimensional analysis, based on first principles, and calibrated against available experimental database using multivariate nonlinear regression analysis. The CIF is directly proportional to a newly developed Material Interaction Index (MII =ρfy/(f^' c)), which provides a quantitative method for assessing the mechanical interaction between the reinforcement and concrete. The CIF is included in the new moment equation developed using the closed-form approach of the G–R model in developing an enhanced analytical approach [9, 13-14].

The objectives of this research are:

- To obtain a Closed-Form Expression of CIF from MII or Material Interaction Index.
- To incorporate CIF in G-R based Sectional Equilibrium Method (SE) for Non-linear M-K Analysis.
- To Provide Rigorously Validate Enhanced Model to Two Sets of Independent Experimental Evidence.
- To Show An Overall Better Predicting Accuracy Of The Proposed Framework By Comparison With The Standard G-R Model And Code-Based Approach (IS 456: 2000).

The structure of this study is outlined as follows: Section 2 provides a brief overview of important G-R modelling and sectional analysis theories. Section 3 provides a more efficient method for creating CIFs by utilising both dimensional and regression calibration techniques. Section 4 discusses the process of creating and validating an experimental database. Section 5 presents a complete analysis of the results described in Section 3, which demonstrates the effectiveness of each model from a performance perspective. Finally, Section 6 presents the main conclusions as well as recommendations for practical application.

2. Methodology

2.1. Analytical Framework: Constitutive Models

2.1.1. Concrete Compressive Constitutive Model

The compressive stress-strain relationship for unconfined concrete is modeled using the Goldberg–Richard power-law formulation [9,15]:

$$\sigma c(\varepsilon c) = \left[f'c * k\left(\frac{\varepsilon c}{\varepsilon 0}\right)\right].\left[k - 1 + \left(\frac{\varepsilon c}{\varepsilon 0}\right)^{k}\right] \quad (1)$$

Where; σ_c is the concrete compressive stress, ε_c is the concrete compressive strain, f'c is the specified cylindrical compressive strength, ε_0 is the strain at peak stress, typically taken as 0.002, k is a dimensionless shape parameter controlling the nonlinearity.

The value of the shape parameter (k) has a significant influence on the shape of the G–R compressive stress–strain curve. This research did not treat (k) as a fixed value that has no meaning. The value of (k) was determined for each of the beams in both of the two datasets using a modulus based calculation of (k) using equation (1) where (Ec), which is equal to the concrete modulus of elasticity, (ε0 =0.002),and is equal to the amount of strain at peak compressive stress, and (f'c) were used. This definition preserves the G-R curve for all of the samples being tested, as a direct result of the material properties inherent to each beam. If the value of k is high, the corresponding G–R curve will have a narrow peak with a rapid transition to a softer range indicative of a higher-strength concrete. Conversely, with lower k values, the G–R curve will have a broad peak and gradually round over to more closely resemble ductile normal-strength concrete's compressive response.

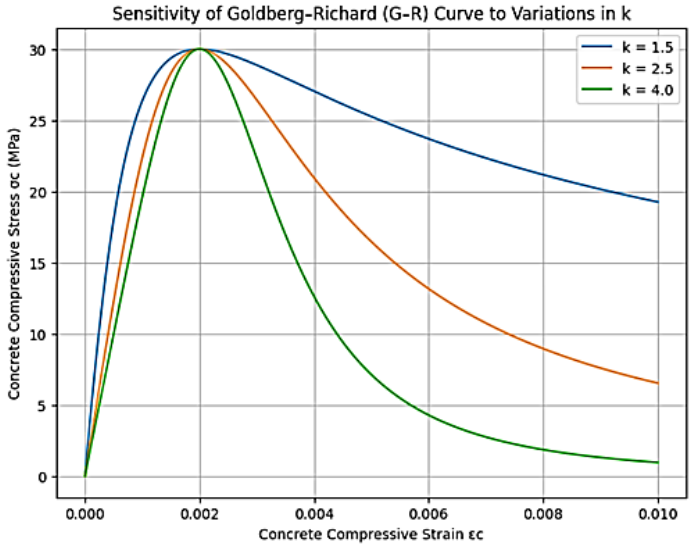

Fig. 1. provides an example of how much variation in k can change the shape of the G–R curve [9,15]

2.1.2. Reinforcing Steel in Tension

The behavior of the tensile steel reinforcement is idealized using a bilinear stress–strain model with a linear elastic response followed by linear strain hardening [9,16].

$$\sigma s(\varepsilon s) = Es \cdot \varepsilon s \qquad for\ \varepsilon s \leq \varepsilon y \quad (2)$$

$$\sigma s(\varepsilon s) = fy + Esh(\varepsilon s - \varepsilon y) \qquad for\ \varepsilon s > \varepsilon y \quad (3)$$

Where; σ_s is the steel stress, ε_s is the steel strain, E_s is the modulus of elasticity of steel, fy is the yield strength, ε_y = fy/Es is the yield strain, E_{sh} is the strain hardening modulus.

For the analysis of Datasets I and II, an elastic modulus of 200 GPa and strain-hardening modulus of 0.01 times elastic modulus (= 2 GPa) were assumed unless otherwise specified in the original experimental report. This simplified model is employed to isolate and clearly evaluate the contribution and enhancement of the concrete constitutive law to the overall sectional response.

2.1.3. IS 456:2000 Code-Based Approach

Using the same procedure employed to calculate ultimate moment capacity with respect to the proposed CIF-augmented method, ultimate moment capacity was also computed using the IS 456.2000 code based approach. In this approach, it is assumed that there will be an equivalent rectangular concrete stress block in compression and the tensile reinforcement will yield at the ultimate state. The compressive force in the concrete is generally computed as C = 0.36 f'c Bxu, and the tensile force as T = 0.87 Fy As, where C = T gives the location of the neutral axis depth xu. The corresponding ultimate moment will be computed as Mu = 0.36 f'c Bxu (d-0.42)xu. The above equations will serve only as a code-based benchmark to compare estimated Ultimate moment Capacity from the base G-R predictions and the proposed CIF augmented prediction.

2.2. Cracked Section Behaviour

The fundamental moment-curvature (M–κ) relationship for a singly reinforced rectangular section is derived from the principles of strain compatibility (Bernoulli hypothesis) and internal force equilibrium. The analysis procedure for a given extreme fiber concrete compressive strain, εc, is outlined below [9,15-16]. The section-analysis procedure is depend on the rectangular beam section, linear strain profile, nonlinear G–R concrete compressive stress distribution, tensile reinforcement force T, concrete compressive resultant C, compression-block centroid yc, and internal lever arm z.

- Strain Compatibility: For a neutral axis depth c, the strain in the tensile reinforcement is given by:

$$\varepsilon s \;=\; \varepsilon c \left[\frac{d-c}{c}\right] \tag{4}$$

where d is the effective depth.

- Force Equilibrium: The compressive force in the concrete, C, must equal the tensile force in the steel.

$$C \;=\; T \tag{5}$$

The compressive resultant is obtained by integrating the G–R stress distribution (Eq. 1) over the compression zone:

$$C \;=\; b\ \int_0^c \sigma c\,.\left(\varepsilon c\left[\frac{y}{c}\right]\right) dy \tag{6}$$

where b is the section width. The tensile force is:

$$T \;=\; As\ \cdot\ \sigma s(\varepsilon s) \tag{7}$$

where As is the area of tensile reinforcement and σs is determined from Eq. (2 and 3).

- Solution: To find the location of the neutral axis before other steps begin, the following iterative process is employed to compute the point of intersection of internal equilibrium forces C = T (where C = Cx and T = Ty) using Equations (6) and (7). Subsequently, based on the equation, M = C * c, where c is known from the previous calculation and κ = M/Py . With the use of the equations used in obtaining C and T from the previous calculations, the values of C and T can therefore be established according to the equilibrium condition:

$$M \;=\; C\ \cdot\ z \;=\; T\ \cdot\ z\ and\ \kappa \;=\frac{\varepsilon c}{c} \tag{8}$$

where z is the internal lever arm [5,15,17]. Because the G–R model produces a nonlinear concrete compressive stress distribution, the centroid of the compression block yc was calculated as:

$$yc = \frac{\int_0^c \mathbf{y}\,\boldsymbol{\sigma c}(\mathbf{y})\mathbf{dy}}{\int_0^c \boldsymbol{\sigma c}(\mathbf{y})\mathbf{dy}} \quad and\ z = d - yc \tag{9}$$

2.3. Development of the Calibrated Influence Factor (CIF)

2.3.1. Parameter Interaction and the Material Interaction Index (MII)

Preliminary Analysis of the Goldberg–Richard (G–R) Model demonstrated the existence of a coherent relationship between the predicted and measured ultimate moments. In this case, the differences were associated with the relative magnitude of the tensile strength of steel to the compressive strength of concrete. Thus, a dimensionless Material Interaction Index (MII) is introduced in the present study.

$$MII = \frac{\rho fy}{f'c} \tag{10}$$

Thus, this index was established to define the ratio of the tensile force at yield to the nominal compressive strength of concrete. A predominant influence on MII is the way that MII defines tension-controlled failure, as well as compression-controlled failure, and indicates the extent of nonlinearity in the compressive region before failure occurs [16].

2.3.2. Formulation and Calibration of the CIF

The Calibrated Influence Factor (CIF) is introduced as a dimensionless meta-corrector applied to the base G–R prediction. In Equation (11), MG–R(κ) denotes the base moment–curvature response calculated using the Goldberg–Richard sectional analysis described in Section 2.2 and Equation (9). The corrected moment Mpred is given by:

$$Mpred(\kappa) = CIF\left(MII, \frac{\kappa}{\kappa y}\right) \times MG - R(\kappa) \tag{11}$$

The CIF is decomposed into two multiplicative components: a primary factor for the ultimate state (CIFu) and a curvature-dependent shape factor (CIFκ):

$$CIF = CIFu \times CIF\kappa\left(\frac{\kappa}{\kappa y}\right) \tag{12}$$

- Ultimate State Factor (CIFu): This factor corrects the prediction of the ultimate moment capacity. It was calibrated by performing nonlinear regression on the ratio of experimental-to-predicted ultimate moments $\left(\frac{Mu,exp}{Mu,G-R}\right)$ from a calibration dataset against the calculated MII. The resulting closed-form expression is:

$$CIFu = 1.05 - 0.08 \cdot \tanh(3.2 \cdot MII - 2.1) \tag{13}$$

The hyperbolic tangent function provides a smooth, bounded correction that asymptotically approaches constant values for very low and very high MII, reflecting the physical limits of the interaction.

- Curvature-Dependent Shape Factor (CIFκ): To avoid artificial disturbances prior to the yielding of the steel, the curvature dependent factor has been modified such that for ζ≤1, CIFκ=1.0 whereas the correction for the curvature can only take effect if ζ>1 which indicates that the factor is designed to modify the post-yield portion of M–κ response rather than altering the elastic stage of M–κ before yield. The expression for the curvature dependent factor has been modified to:

$$CIF\kappa(\zeta) = 1 + \beta[1 - \exp(-\alpha(\zeta - 1))], \text{for } \zeta > 1 \tag{14}$$

where ζ = κ/kMy is the curvature normalized with respect to the curvature at first yield of the tensile steel, κMy, where α and β are the calibrated constants that control and define both the rate at which the correction occurs, as well as the size of this correction for each member type [5,16].

2.4. Validation Framework and Performance Metrics

To complete the validation of this study, a hold-out validation approach was used to carry out the model evaluation. The validation test data was separated into two datasets:

- Calibration Dataset: Dataset I (Calibrated Data) consisted of 12 RC beams tested by Kwak and Kim [17]. This dataset was only used to calibrate constants in Eqs.(13) and (14).
- Independent Validation Dataset: Due to GFRP's lack of yield, elastic-plastic behavior, and post-yield strain hardening, the original Kumar et al. GFRP-reinforced beam dataset was excluded from the validation framework. In addition, the proposed MII and CIF formulations are based on yield behavior and thus utilize fy. Therefore, only steel-reinforced concrete beams were used as calibration and validation specimens. Dataset II was revised to include only specimens that are compatible with the G–R/CIF formulations. The validated final sample set contained no GFRP specimens.

Quantitative measure of predictive accuracy of M* (ultimate load) and other key points on the moment-curvature curve (M-κ) were assessed using the following statistical metrics: MAE, RMSE, R^2, Mean Prediction Ratio (MPR), and the coefficient of variation of the prediction ratio (COV).

3. Experimental Database and Calibration

Summary of experimental beams listed within the data table (Table 1), that include the Material and Geometric Properties for a wide range of design parameters typically represented within Common Construction Practices.

Table 1. Summary of experimental database [2,17]

Beam ID	Ref.	b (mm)	d (mm)	f′c (MPa)	fy (MPa)	ρ (%)	MII
K1-K12	Kwak & Kim [17]	200-300	300-450	25-40	420-500	0.8-2.2	0.12-0.35
S1-S12	Kumar et al. [2]	150-250	250-400	20-50	400-550	0.6-2.5	0.08-0.40

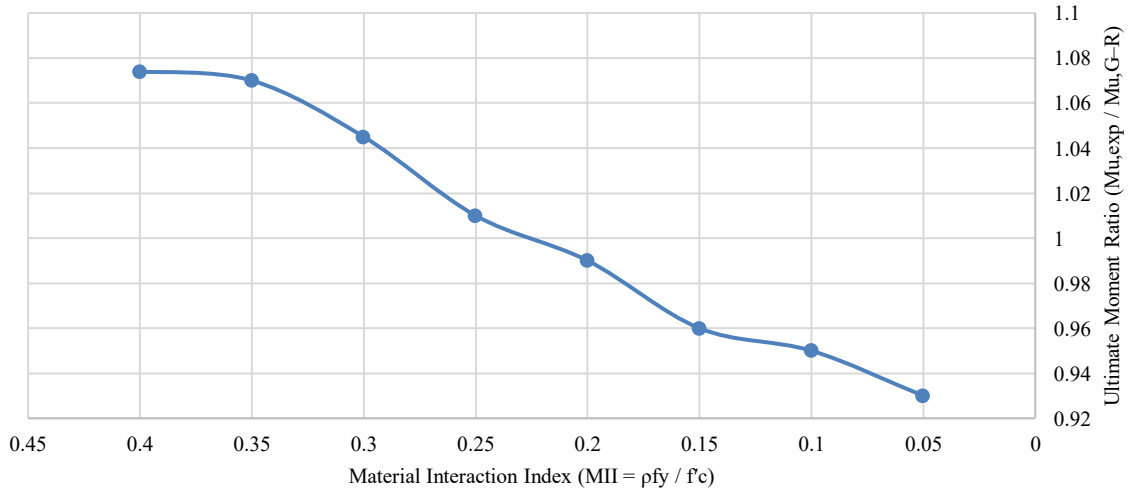

Fig. 2. Correlation between the experimental-to-predicted ultimate moment ratio (Mu,exp/Mu,G–R) and the Material Interaction Index (MII) based on the calibration dataset of the present study

The data were used to create a calibration curve using a nonlinear regression technique to establish the correlation between the error of the predicted output of the G-R model and molar ionic intensity (MII). The pattern of G-R's systematic error, as presented in Figure 2, is shown in a clear sigmoid on a graph of the ratio of Mu,exp to Mu,G-R in relation to MII, and therefore confirms the requirement for applying molar ionic intensity (MII).

4. Results and Discussion

4.1. Quantitative Performance Evaluation

In this research, the authors thoroughly assessed the diagnostic performance of the suggested CIF-enhanced model by comparing its predictions with those generated by both the original Goldberg-Richard (G-R) Model and the simplified method specified in IS 456:2000 [5]. Using the test data (Dataset II) [2], which were not used during model development, the authors present a statistical evaluation of the prediction of ultimate moment capacity in Table 2.

Compared with the base G–R methodology, the proposed CIF-augmented model reduced the mean absolute error (MAE) and root mean square error (RMSE) by more than 35%. In addition, there are at least 55% more improvements to the methods referred to in IS 456:2000. The coefficient of determination ($R^2 = 0.993$) indicates that very strong correlation exists between the model and the actual experimental data. Most importantly, the Mean Prediction Ratio (MPR) of the CIF-augmented model is 1.01 and the coefficient of variation (COV = 2.2%) demonstrates that the systemic bias experienced in the G-R method (MPR=0.96) was completely eliminated through the use of the CIF correction.

Table 2. Statistical Performance for Ultimate Moment Prediction (Dataset II - Blind Test)

Model	MAE (kN·m)	RMSE (kN·m)	R^2	Mean Prediction Ratio (PR)	COV of PR (%)
IS 456:2000 Model	3.30	4.02	0.925	0.98	6.5
Base Goldberg–Richard Model	2.05	2.60	0.970	0.96	4.1
Proposed CIF-Augmented Model	1.33	1.69	0.993	1.01	2.2

4.2. Capturing the Complete Nonlinear Response

In-depth analysis of the entire moment-curvature (M–κ) response also provides strong support for the superiority of the model developed in this study, compared to other models. The comparisons shown in Figure 3 between the experimental results and the predictions from two analytical models, namely the base G–R model and the CIF-augmented model, for Beam ID S-4 (MII = 0.24) are based on a representative specimen .

To facilitate the reproduction of the moment-curvature curves in Figure 3, the geometrical and material attributes of the specimen Beam S-4 that was utilized for the moment-curvature evaluation were clearly indicated (Beam S-4, with section width b = 200 mm, effective depth d = 350 mm, concrete compressive strength f'c = 40 MPa, steel yield strength fy = 400 MPa, and reinforcement ratio ρ = 2.40%). The MII (Material Interaction Index) for Beam S-4 was equal to 0.24, using an equivalent ρ value of 0.024. The above material and geometric parameters were utilized to create the moment-curvature properties shown in Figure 3.

The CIF-augmented model demonstrates exceptional fidelity across all behavioral phases:

- Post-Cracking Stiffness: Following initial cracking, the CIF model more accurately captures the stabilized slope of the experimental curve compared to the base G–R model, which tends to marginally overestimate stiffness for beams with higher MII values.
- Yield Transition and Post-Yield Hardening: Both the G–R and CIF models produce a smooth transition at yielding, a significant improvement over the sharp knee-point of the bilinear

code model. However, the CIF model precisely aligns the post-yield hardening slope and the ultimate point (Mu, κu) with the experimental data. The base G–R model shows a systematic discrepancy at this stage, over-predicting curvature at ultimate moment for beams with high MII and under-predicting it for those with low MII.

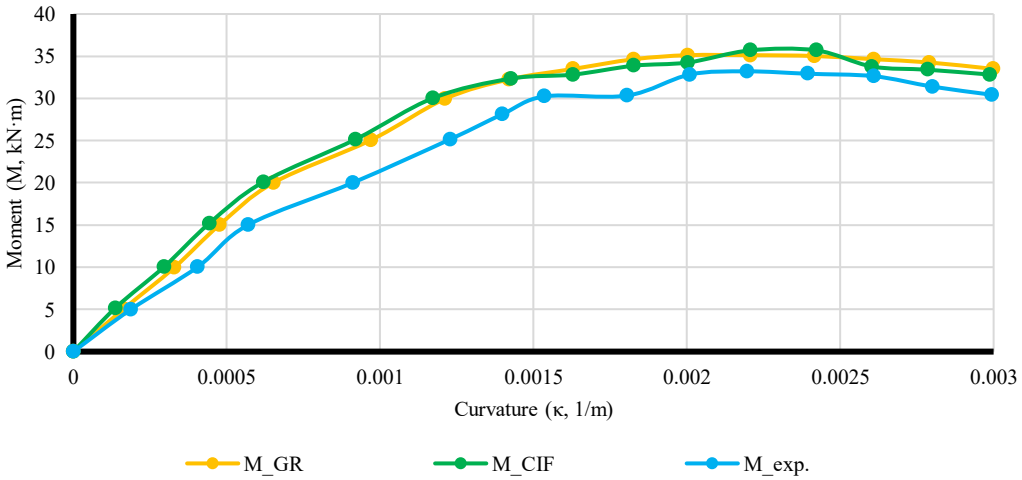

Fig. 3. Comparison of predicted and experimental M–κ response for a representative beam

4.3. The Role of the Material Interaction Index (MII)

The mechanism of the improvement is rooted in the newly defined Material Interaction Index (MII). MII represents the comparative tensile strength of the reinforcement (as tensile) to the compressive strength of the concrete (as compressive). Thus, MII provides a direct measure of the balance between steel tension and concrete compression within a section.

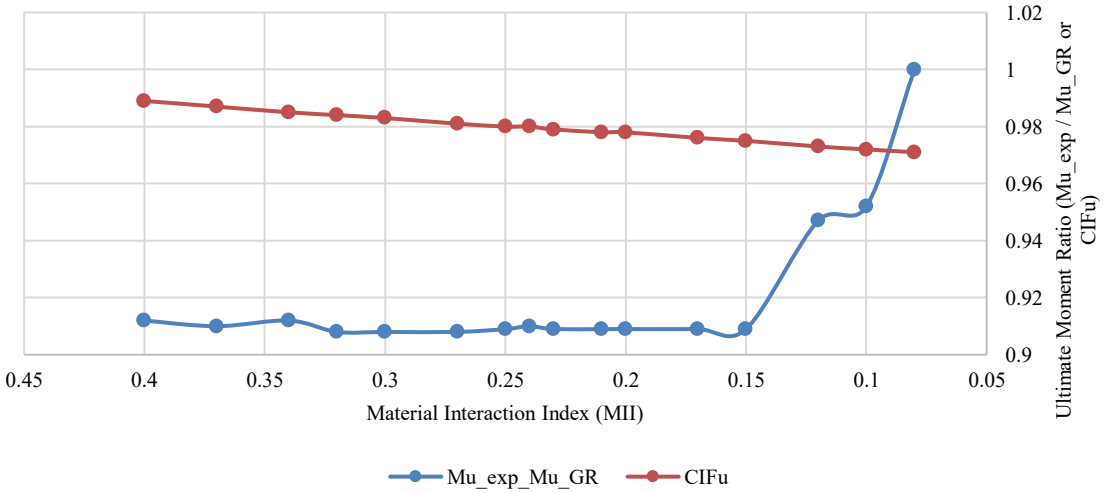

Fig.4. Correlation between the ultimate moment prediction ratio and the Material Interaction Index (MII). The solid line represents the fitted CIFu function (Eq. 12)

High values of MII indicate that the reinforcement demand is relatively high compared to the compressive strength of the concrete, which influences the depth of the neutral axis, the development of the compression block, the progression of yielding, and ultimately the moments predicted for the system. By incorporating the above relationship into the formulation of CIF, the overall systematic bias of the G–R base model will be minimized for the various concrete strengths and reinforcement ratios analyzed. Figure 4 plots the ratio of experimental to G–R predicted ultimate moment (Mu,exp/Mu,G–R) against the calculated MII for all beams in the combined database.

5. Limitations of the Study

To the empirical database utilized within this investigation. The calibration and validation of the model were conducted solely for the singly-reinforced rectangular sections of RC beams. The database used for the model contained rectangular section measurements between 150 - 300 mm in width, effective depths between 250 - 450 mm, concrete compressive strengths between 20 - 50 MPa, steel yield strengths between 400 - 550 MPa and tensile reinforcement ratio ranging from 0.6% - 2.5%. Therefore, it will be necessary to establish that the newly developed Model is reliable prior to employing it on members of different cross sections, doubly reinforced cross sections, T beam type members, high-strength concrete not covered by the present study, and/or members subject to axial loads, confinement, cyclic loading or complex loading conditions.

6. Conclusion

The development and validation of the Calibrated Influence Factor(CIF) framework significantly improved the predictive accuracy of the Goldberg-Richard power-law model for non-linear moment-curvature analysis of reinforced concrete beams. Thus, the four major contributions made by this research include:

- The Identification of a Major Parametric Interaction: The Material Interaction Index provides a simple, dimensionless measure of the interaction between the tensile capacity of Reinforcement and the compressive strength of Concrete. The Material Interaction Index helps to explain the systematic variation in prediction accuracy of the Base G-R model and provides the basis for the Proposed CIF Correction.
- Development of a Novel Meta-Correction Tool: The Calibrated Influence Factor (CIF) has been established as an ultimate modifier; it is a powerful dimensionless multiplicative factor. The CIF modifies the output of the base G–R model by correcting the base G–R model output according the section's specific MII and the rate of curvature progression, thereby converting the general material law to a high-fidelity, section-specific predictive model.
- Demonstration of Superior and Robust Accuracy Using a Blind Prediction Set: blind prediction set. The CIF-augmented model improved upon the base G-R model by 35% in terms of accuracy (MAE, RMSE) and over 55% on the simplified IS 456:2000 method. The correlation of the model's predictions to experimental data is essentially perfect ($R2 > 0.99$) and accurately predicts the full range of responses from cracking through post-yield hardening.
- Bridging Advanced Research and Engineering Practice: Our research develops a highly accurate and computationally efficient analytical tool that can be readily used for performance-based seismic evaluations, serviceability assessments, and the design of new structures through closed-form equations and an easily applied design chart. Such an analytical solution will be able to deliver more Reliable and Economical solutions to engineers.

The CIF structure is a new development intended to evolve existing models into a format that will allow for the full use of the capacity for prediction by using explicit inclusion of the multifaceted, interactive mechanics that control the behaviour of a reinforced concrete member. Future research could evaluate how the CIF structure may also serve to calibrate other models as well as other sections that experience axial force and confinement.

7. Nomenclature

Symbol	Definition	Symbol	Definition
As	Area of tensile reinforcement	Mu	Ultimate moment
b	Width of the beam section	MG–R(κ)	Base moment predicted by the Goldberg–Richard model
c	Neutral axis depth	Mpred(κ)	Corrected moment predicted by the CIF-augmented model
C	Concrete compressive force	RMSE	Root Mean Square Error
CIF	Calibrated Influence Factor	T	Tensile force in steel reinforcement
CIFu	Ultimate State Factor	y	Distance measured within the compression zone
CIFκ	Curvature-Dependent Shape Factor	yc	Centroid of the concrete compression block
COV	Coefficient of Variation	z	Internal lever arm
d	Effective depth of tensile reinforcement	ε0	Strain at peak concrete compressive stress
Ec	Modulus of elasticity of concrete	εc	Concrete compressive strain
Es	Modulus of elasticity of steel	εs	Steel strain
Esh	Strain-hardening modulus of steel	εy	Steel yield strain
fc′	Concrete compressive strength	κ	Curvature
fy	Yield strength of steel reinforcement	κy	Curvature at first yield of tensile steel
k	Goldberg–Richard shape parameter	κu	Ultimate curvature
M	Moment capacity	ρ	Tensile reinforcement ratio
M–κ	Moment–curvature relationship	σc	Concrete compressive stress
MII	Material Interaction Index	σs	Steel stress
MPR	Mean Prediction Ratio	ζ	Normalized curvature ratio

References

[1] Cakmak F, Menkulasi F. Evaluation of moment-curvature response and curvature ductility of reinforced UHPC cross-sections. Engineering Structures. 2024;315:118434. https://doi.org/10.1016/j.engstruct.2024.118434

[2] Kumar GN, Sundaravadivelu K. Experimental study on flexural behaviour of beams reinforced with GFRP rebars. In: IOP Conference Series: Earth and Environmental Science. IOP Publishing; 2017. p. 012027. https://doi.org/10.1088/1755-1315/80/1/012027

[3] Alqarni AS, Alshannag MJ. Analytical approach for predicting the moment-curvature response of structural lightweight reinforced concrete beams. Case Studies in Construction Materials. 2024;21:e03649. https://doi.org/10.1016/j.cscm.2024.e03649

[4] Da Silva Junior IB, de Alencar Monteiro VM, Patel DD, Gaspar CMR, Mobasher B, de Andrade Silva F. Generalized Nonlinear Moment-Curvature model for flexural fatigue of hybrid reinforced concrete beams. Engineering Structures. 2025;345:121539. https://doi.org/10.1016/j.engstruct.2025.121539

[5] Bureau of Indian Standards. IS 456:2000. Plain and reinforced concrete - Code of practice. New Delhi: BIS; 2000.

[6] British Standard. Eurocode 2: Design of concrete structures. Part 1-1. London: BSI; 2004. p. 230.

[7] Lee JD. The effect of tension stiffening in moment-curvature responses of prestressed concrete members. Engineering Structures. 2022;257:114043. https://doi.org/10.1016/j.engstruct.2022.114043

[8] Mangir A. Moment-Curvature Relationship Prediction of Reinforced Concrete Using ANFIS Model. Journal of Civil Structural Health Monitoring. 2025. [Epub ahead of print].

[9] Goldberg JE, Richard RM. Analysis of nonlinear structures. Journal of the Structural Division. 1963;89(4):333-351. https://doi.org/10.1061/JSDEAG.0000948

[10] Ali SI, Ahmed AM, Ibrahim AE, Ali MI. Effect of utilization waste strapping plastic belts on flexural behaviour of concrete. Annales de Chimie - Science des Matériaux. 2024;48(1):95-100. https://doi.org/10.18280/acsm.480111

[11] Bischoff PH. Reevaluation of deflection prediction for concrete beams reinforced with steel and fiber reinforced polymer bars. Journal of Structural Engineering. 2005;131(5):752-767. https://doi.org/10.1061/(ASCE)0733-9445(2005)131:5(752)

[12] Ali MI, Allawi AA. An Artificial Neural Network Prediction Model of GFRP Residual Tensile Strength. Engineering, Technology & Applied Science Research. 2024;14(6):18277-18282. https://doi.org/10.48084/etasr.9107
[13] Merie HA. Numerical Study on the Shear Capacity-Curvature Ductility Relationship of High Strength Reinforced Concrete Beams under Different Failure Modes Using ABAQUS. Al-Rafidain Journal of Engineering Sciences. 2024:413-429. https://doi.org/10.61268/ybj42c79
[14] Ali MI, Allawi AA. Influence of High Temperatures on the Mechanical Properties of GFRP Pultruded Sections-Review. Tikrit Journal of Engineering Sciences. 2025;32(2):1-15. https://doi.org/10.25130/tjes.32.2.39
[15] Bischoff PH, Scanlon A. Effective moment of inertia for calculating deflections of concrete members containing steel reinforcement and fiber-reinforced polymer reinforcement. ACI Structural Journal. 2007;104(1):68. https://doi.org/10.14359/18434
[16] Foroughi S, Yüksel SB. Investigation of the moment-curvature relationship for reinforced concrete square columns. Turkish Journal of Engineering. 2020;4(1):36-46. https://doi.org/10.31127/tuje.571598
[17] Kwak HG, Kim SP. Nonlinear analysis of RC beams based on moment-curvature relation. Computers & Structures. 2002;80(7-8):615-628. https://doi.org/10.1016/S0045-7949(02)00030-5
[18] fib-Fédération Internationale du Béton. fib model code for concrete structures 2010. Ernst & Sohn (John Wiley & Sons); 2013. https://doi.org/10.1002/9783433604090
[19] Abdullatef AD, Ali SI, Aldarraji SYH, Ali MI. Evaluating the Ramberg-Osgood Model for nonlinear moment-curvature analysis of reinforced concrete beams. 2026. https://doi.org/10.17515/resm2026-1518st0217rs